Zebrafish mesonephric renin cells are functionally conserved and comprise of two distinct morphological populations

Zebrafish mesonephric renin cells are functionally conserved and comprise of two distinct morphological populations.

Sebastien A. Rider[1], Helen C. Christian[2], Linda J. Mullins[1], Calum A. MacRae[3] and John J. Mullins[1]

[1]University/BHF Centre for Cardiovascular Science, The Queen's Medical Research Institute, Little France, The University of Edinburgh, Edinburgh, EH16 4TJ. [2]Department of Physiology, Anatomy and Genetics, Le Gros Clark Building, South Parks Road, Oxford, OX1 3QX. [3]Cardiovascular Division, Department of Medicine, Brigham and Women's Hospital and Harvard Medical School, Boston, MA, 02115.

Correspondence: Dr Sebastien Rider, University/BHF Centre for Cardiovascular Science, The Queen's Medical Research Institute, Little France, The University of Edinburgh, Edinburgh, EH16 4TJ. Phone: (+44) 0131 242 26729. Fax (+44) 0131 242 9101. Email: srider@staffmail.ed.ac.uk

Running Title

Distinct morphologies of mesonephric renin cells

Abstract

Zebrafish provide an excellent model in which to assess the role of the renin-angiotensin system in renal development, injury and repair. In contrast to mammals, zebrafish kidney organogenesis terminates with the mesonephros. Despite this, the basic functional structure of the nephron is conserved across vertebrates. The relevance of teleosts for studies relating to the regulation of the renin-angiotensin system was established by assessing the phenotype and functional regulation of renin-expressing cells in zebrafish.

Transgenic fluorescent reporters for renin (*ren*), smooth muscle actin (*acta2*), and platelet derived growth factor receptor beta (*pdgfrb*) were studied to determine the phenotype and secretory ultrastructure of perivascular renin-expressing cells. Whole-kidney *ren* transcription responded to altered salinity, pharmacological renin-angiotensin system inhibition, and renal injury.

Mesonephric *ren*-expressing cells occupied niches at the pre-glomerular arteries and afferent arterioles, forming intermittent epithelioid-like multi-cellular clusters exhibiting a granular secretory ultrastructure. In contrast, renin cells of the efferent arterioles were thin-bodied and lacked secretory granules. Renin cells expressed the perivascular cell markers *acta2* and *pdgfrb*. Transcriptional responses of *ren* to physiological challenge support the presence of a functional renin-angiotensin system and are consistent with the production of active renin.

The reparative capability of the zebrafish kidney was harnessed to demonstrate that *ren* transcription is a marker for renal injury and repair. Our studies demonstrate substantive conservation of renin regulation across vertebrates and ultrastructural studies of renin cells reveal at least two distinct morphologies of mesonephric perivascular *ren*-expressing cells.

Key words

Renin, perivascular, renin-angiotensin system, kidney injury, zebrafish.

Introduction

Renin-expressing cells are anatomically restricted to the juxtaglomerular apparatus (JGA) of the adult mammalian metanephros and secrete active renin, the initiating enzyme of the renin-angiotensin system (RAS). The RAS principally functions to maintain cardiovascular homeostasis. In humans, over-stimulation of RAS is associated with clinical hypertension and an increased risk of chronic kidney disease (CKD) (76). Over-production of angiotensin II (ANG II), the effector of the RAS, may be pharmacologically targeted by angiotensin-converting enzyme (ACE) inhibitors or

angiotensin receptor blockers (ARBs) (78). Renin-expressing cells of the developing metanephros are widespread throughout the nascent renal vasculature, yet their role remains poorly understood (19, 20, 62). In the embryo, renin cells may secrete active renin for RAS-mediated homeostasis or developmental pathways and (42), as activated pericytes, may be required for renal angiogenesis (56, 58, 77).

The canonical RAS first appeared in teleosts and perivascular *ren*-expressing cells are conserved in larval zebrafish (14, 38). A complete understanding of their functional relationship across vertebrates is, however, lacking. The intracellular granules of renin cells, only partially characterised in teleosts (8, 32, 33, 50), are fundamental to the synthesis and release of active renin. Fully differentiated renin cells of the mammalian juxtaglomerular apparatus (JGA) contain a large number of acidic secretory granules that process prorenin into its active form for regulated secretion (71). Mammalian renin cells present during development (72), or those recruited in response to homeostatic challenge (66), exhibit an intermediate phenotype with smaller and sparser renin granules.

The teleost kidney allows modelling of both nephron repair and regeneration post-injury (13, 43, 86). The final-stage kidney of adult zebrafish, the mesonephros, retains a nephron progenitor population throughout life and continually undergoes *de novo* nephrogenesis (61, 86). Tubular injury is expected to activate the RAS as a result of impaired solute uptake or nephron filtration (31). Post renal injury, the RAS and renin pericytes may be activated for tubular repair and *neo*-nephrogenesis (21, 45, 65). Current evidence suggests that renin cells belong to a pericyte lineage, but their differentiation pathways remain to be fully elucidated (7, 70). In mammalian experimental disease models, cells of renin lineage (CoRL) are multipotent and capable of repopulating multiple glomerular cell niches, including *pdgfrb* expressing mesangial cells (54, 55, 68).

The aims of the present study in adult zebrafish were to assess the functional and phenotypic conservation of renin-expressing cells in a lower vertebrate. We used transgenic reporter fish and

physiological challenges to address several questions. 1) Where are renin-expressing cells localised in adult zebrafish? 2) Do renin-expressing cells express markers of smooth muscle cells and pericytes? 3) Is their intracellular structure reminiscent of mammalian JGA cells that secrete active renin enzyme? 4) Are the physiological roles of renin-expressing cells consistent with a functional RAS? Our data establish the zebrafish model for studies of the RAS and its role in kidney injury and repair.

Methods

Fish lines and husbandry

Experiments were approved by the local ethics committee and conducted in accordance with the Animals (Scientific Procedures) Act 1986 in a UK Home Office approved establishment. Zebrafish (*Danio rerio*) were maintained at 28.5 °C, as described by Westerfield (58, 80). Established lines used included WIK, *casper* (81), tg(*ren*:LifeAct-RFP) (58), tg(*kdrl:*EGFP) (11), tg(*wt1b:*EGFP) (52), and tg(*acta2*:EGFP) (82). Adult fish were anaesthetised with 40 μg ml^{-1} tricaine methanesulfonate (MS-222). All fish used in this study were 10-12 months of age. For all experiments fish were individually housed in one litre tanks in solutions adjusted to pH 7.6. For experiments longer than 24 hours, fish were fed daily, otherwise feed was withheld.

Generation of tg(pdgfrb:EGFP) fish

A 7.16 kb region upstream of the *pdgfrb* translational initiation site was isolated from WIK genomic DNA using the following primer sequences with *attB* sites for gateway recombination into pDONR4-PIR (Invitrogen); *pdgfrb* forward 5'-GGGGACAACTTTGTATAGAAAAGTTGCTTCTCAGGCTCTATCAAGTTGGATGG; *pdgfrb* reverse 3'-GGGGACTGCTTTTTTGTACAAACTTGCTCAACACTGCAGACGGAGAGAAAAC. The DNA fragment was recombined upstream of EGFP and SV40 polyA sequences by three-way gateway cloning into pDestTol2CG2 (containing minimal *tol2* ends and *cardiac myosin light chain*:EGFP) of the tol2 system (37). Plasmid DNA was co-injected with transposase mRNA transcribed in-house. Fish with visible

pdgfrb-EGFP fluorescence displayed similar expression patterns to those previously reported (3, 79, 83).

In situ hybridisation (ISH)

Whole adult fish were fixed in 4% PFA and processed into paraffin embedded sagittal sections. ISH was conducted using standard protocols (58, 75). Briefly, a 500 bp digoxigenin (DIG)-labelled RNA probe was synthesised from *ren* cDNA. Embryos were rehydrated, permeablised, and incubated at 65 °C for 16 hrs in hybridisation buffer. Following hybridisation, DIG-labelled RNA probes were detected with an alkaline phosphatase conjugated anti-DIG antibody (Roche) visualised by reaction with 5-bromo-4-chloro-3-indolyl phosphate and nitro blue tetrazolium (NBT). Sections were counter-stained with methyl green. *Ren* mRNA was only detected in the renal tissue.

Intracellular acidic granule staining

Whole kidneys from tg(*ren*:LifeAct-RFP, casper) were excised into Dulbecco's Modified Eagle's medium (DMEM) with 5 µM Lysotracker® Green DND-26 (Molecular Probes™) for 1 hr at room temperature. Kidney tissue was then prepared by kidney squash for immediate confocal imaging of *ren*:LifeAct-RFP expressing cells.

Electron microscopy and ren:LifeAct-RFP immunogold

Prior to fixation, renal tissue was dissociated from haematopoietic cells by trituration in DMEM. Renal tissue was recovered with a 40 µm cell strainer. Samples were prepared for standard and *ren*:LifeAct-RFP immunogold electron microscopy (EM) by standard methods (1). Briefly, for immunogold EM, segments were stained with uranyl acetate (2% w/v in 0.1 M sodium acetate buffer), dehydrated through increasing concentrations of methanol (70-100%) at -20 °C and embedded in LR Gold (London Resin Company, Reading, UK). Ultrathin sections (50-80 nm) were prepared using a Reichert ultracut S microtome and mounted on 200 mesh nickel grids. Sections were incubated at room temperature for 2 hr with anti-RFP (Clontech, Mountain View, CA, USA

dilution 1:1000) and for 1 hr with anti-rabbit IgG-15 nm gold complex (dilution 1:50; BBI, Cardiff UK). All antisera were diluted in 0.1 M phosphate buffer containing 0.1% egg albumin. As a secondary antibody negative control the primary antibody was replaced by phosphate buffer/egg albumin and no labelling was observed. After immunolabelling, sections were lightly counterstained with lead citrate and uranyl acetate and examined with a JEOL transmission electron microscope (JEM-1010, JEOL, Peabody, MA, USA) fitted with an Orius digital camera (GATAN, CA, USA).

Kidney tissue RNA analysis

Kidney samples were excised either whole or with the head kidney separated from the trunk and tail regions (Fig 1A). Tissue was immediately frozen on dry ice and stored at -80 °C until analysis. Total RNA was extracted from kidney tissue in TRIzol® (Ambion) reagent using a Qiagen RNeasy kit (Qiagen) according to the manufacturer's instructions. RNA samples were quantified using a NanoDrop (Thermo Scientific) and integrity analysed by gel electrophoresis. RNA (500 ng) was reverse transcribed using a High Capacity cDNA Reverse Transcription Kit (Applied Biosystems™) and real-time PCR performed with the Universal Probe Library (UPL) system from Roche Diagnostics Ltd., using a Roche Lightcycler 480 (Roche, West Sussex, UK). Primers were designed and utilised with the Roche Universal Probe Library (Table 1). Gene expression was normalized to the mean expression of ribosomal protein S18 (*rps18*) and elongation factor 1 alpha (*eef1a1*).

Salinity challenge and captopril treatment

Fish were exposed to various saline solutions for a 24 hour period (n = 8). As similarly described (25, 59), 1x conditioned water (CW) contained 60 mg l^{-1} marine salts (Tropic Marin®), 1/10th CW contained 6 mg l^{-1} marine salts, and 10x Na & K contained 1x CW supplemented with 365 µM KCl and 171 mM NaCl. 0.05 mM waterborne captopril (C4042, Sigma-Aldrich) was administered in 1x CW for four days (n=10).

Kidney injury and regeneration with captopril treatment

For the induction of tubular injury, fish were intraperitoneally injected with either 65 mg/kg gentamicin or PBS for sham fish using a 10 µl NanoFil Syringe with a 35 gauge needle. Transcriptional responses to kidney injury were determined 48 hours post-injection. For the analysis of regeneration, fish were sampled eight days post injection. The effects of RAS inhibition on regeneration were determined with 0.05 mM waterborne captopril from 24 hours post gentamicin injection until sampling. Only fish that responded significantly to captopril treatment were included for further analysis, i.e. those with a mean relative *ren* expression at or above that of the control fish. For all other groups $n = 8$.

Kidney regeneration and spatial analysis of kidney ren

Fish were subjected to an intraperitoneal dose of either 75 mg/kg gentamicin or PBS for sham fish. Post-recovery, fish were individually housed in one litre tanks and fed daily. Head, or tail and trunk kidney regions were sampled for RNA analysis nine days post gentamicin injection. Fish not responding significantly to gentamicin, i.e. those with a mean relative *wt1* expression at or below that of the mean of sham fish were excluded from further analysis. Control group $n = 7$.

Confocal imaging

Kidney squashes were prepared using fresh tissue in DMEM or fixed tissue (4% PFA in PBS). For fixed tissue, 300 nM DAPI was diluted in PBS for nuclear staining. Confocal images were taken with a Leica SP5 using a 63x or 100x objective, 3x averaging, and a 0.5 µm z-step size for z-stacks. Optical thickness ranged between 0.5-1 µm. Maximal intensity projections were created with Fiji. Brightfield ISH images were taken using an Olympus Provis AX70 microscope.

Statistical analysis

Statistical analyses were performed with GraphPad Prism 6 (La Jolla, CA). Differences in means between two treatments were analysed by an independent samples t-test. Means between three or more groups were subject to a One-way ANOVA and where appropriate followed by a *post-hoc*

Bonferroni test for comparisons between predetermined treatments groups. Means are reported with a standard error of the mean and *p* values <0.05 were considered significant.

Results

Renin cell localisation and morphology

Visualisation of *ren*:LifeAct-RFP and *ren in situ* hybridisation (ISH) confirmed the location of renin-expressing cells in adult zebrafish. ISH showed *ren* mRNA is specifically associated with the mesonephric vasculature and not detectable in glomeruli, tubular epithelium, or haematopoietic cells (Fig. 1*A*-C), as characteristic of the developing mouse metanephros (26). The *ren*:LifeAct-RFP transgene is *bona fide* for endogenous *ren* in adults and larval fish (58). Despite an even distribution of nephrons across the mesonephros, *ren*:LifeAct-RFP (Fig. 1*D*) and *ren* mRNA transcripts are spatially varied across the kidney, being markedly reduced in the head kidney compared to the trunk and tail regions (Fig. 7).

Crossing tg(*ren*:LifeAct-RFP) to tg(*kdrl:*EGFP), which have endothelial cells labelled with EGFP (11), confirmed the perivascular location of renin cells. Renin is not detectable in the endothelial cells, which is consistent with the distinct lineage of larval zebrafish renin cells to haemangiobalsts and endothelial cells (58). Renin is also not detectable in the endothelium of adult fish. *ren*:LifeAct-RFP was detected in 1) afferent arterioles, at or close to the vascular pole entering the glomerulus, termed the juxtaglomerular (JG) region 2) in the pre-glomerular arteries 3) in the efferent arterioles (Fig. 1*E-H*). Branches of pre-glomerular arteries were present both with and without *ren*:LifeAct-RFP (Fig. 1*F*). As similarly reported in the developing mammalian metanephros (26, 62), renin reporter expression at the afferent arterioles and pre-glomerular arteries was circumferential and discontinuous (Fig. 1*E, H*, *K*). In contrast, expression at efferent arterioles was continuous (Fig. 1*E, H, K*).

The use of LifeAct to direct RFP to filamentous actin (F-actin) allowed for the visualisation of intracellular myofilaments (60), and increased RFP labelling in thin-bodied mural cells. Renin-expressing cells of the pre-glomerular arteries and JG cells formed multicellular epithelioid-like cell clusters composed of tens of cuboidal shaped cells (Figs. 1*I, K* & 2*K*). Conversely, efferent *ren*:LifeAct-RFP expressing cells, displayed flattened cell bodies thinly covering arterioles (Figs. 1*J-K &* 2*J*), as similarly observed in the pectoral arteries of larval fish (58). Regardless of morphology, as reported in other fish species, perivascular renin cells were always comprised of a single cell layer (Figs. 1*I &* 2*K*) (33).

Smooth muscle and pericyte markers in renin cells.

The relationship of renin-expressing cells to smooth muscle cells (SMC) expressing (*acta2*) and pericytes expressing (*pdgfrb*) was analysed using tg(*ren*:LifeAct-RFP, *acta2:*EGFP) and tg(*ren*:LifeAct-RFP, *pdgfrb:*EGFP) fish, respectively. With an inverse relationship to smooth muscle actin (SMA), mammalian renin expression increases along metanephric afferent arterioles with decreasing distance from the glomerulus (35, 36, 48, 62). In zebrafish, all renin-expressing cells co-expressed *acta2:*EGFP (Fig. 2*A-F*) and no inverse relationship between *acta2* and *ren* was evident. Occasional cell clusters at non-specific vascular locations expressed a lower acta2:EGFP (Fig. 2*F*), which may represent nascent renin cells acquiring a SMC phenotype during maturation (40). SMCs between renin cell clusters had thinner cell bodies than epithelioid *ren*-expressing cells (Fig. 2*C-E*). Expression of mammalian pericyte markers *NG2* and *CD146* precede *αSMA* during embryonic renin cell differentiation (69). The expression of *pdgfrb*:EGFP in epithelioid renin cells (Fig. 2*G-I*) suggests that as observed in mammals, zebrafish mesonephric renin cells maintain a functional relationship with pericytes (69).

Renin cell intracellular structure

The intracellular structure of *ren*:LifeAct-RFP -expressing cells was assessed by immunogold electron microscopy and lysotracker green. The acidic milieu of mammalian renin granules is thought to be

required for the activation of prorenin by cleavage of its pro segment to active renin (84). To test for the presence of acidic granules in fish, *ren*:LifeAct-RFP -expressing cells were stained with the acidotrophic dye lysotracker green, which stains lysosomes and other intracellular acidic organelles. Acidic granules were present in renin-cell clusters at both the afferent arterioles and pre-glomerular arteries (Fig. 3*A*-*B*). By comparison, very few acidic organelles were observed in the efferent arterioles (Fig. 3*C*).

F-actin visualised in *ren*:LifeAct-RFP -expressing cells was most prominent at the luminal side of the cells, and to a lesser extent at renin-cell to renin-cell boundaries (Fig. 2*B*-*E*). Mammalian renin cells with an intermediate SMA and renin phenotype contain visible myofilaments, which are difficult to detect in fully differentiated cells of the JGA (22, 73).

Immunogold stained *ren*:LifeAct-RFP cells contained either a highly vacuolated structure with small 50-200 nm electron dense granules of various sizes, or a cytoplasm packed with numerous uniformly sized electron dense granules. As with mammalian renin cells, different intracellular structures suggest different stages of cell maturity. Renin cells (Fig. 4*A*-*D*) with a more vacuolated structure are believed to be representative of an immature endocrine structure. The partially filled protogranules (Fig. 4*B*) and paracrystaline granules (Fig. 4*C*) observed in zebrafish renin cells are also reported in immature mammalian counterparts (74). Cells with highly packed granules (Fig. 4*E*-*H*), ranging from 150-400 nm in size, are expected to represent a fully endocrine renin-secreting cell. Renin granules in zebrafish are similar to the mean 230 nm size of carp renin granules (32). No large mammalian-like granules (approximately 500 nm in size), are present in the zebrafish kidney (71).

Physiological challenge and ren transcription

In mammals, low sodium (23, 85), or RAS inhibition by ACE inhibitors (18, 36, 66), both increase renin transcription, plasma renin activity, and renin cell distribution down the afferent arteriole (17, 41).

RAS inhibition blocks the ANG II-mediated homeostatic negative feedback mechanism that supresses renin secretion (22). Consistent with a functional RAS, our data show that *ren* is upregulated by both captopril and decreasing salinity (Fig. 5), as reported in larval zebrafish (25, 58). This supports a RAS-mediated sodium homeostasis in adult zebrafish. In mammalian whole kidney, upregulation of renin transcription results from renin cell recruitment, or upregulation within individual cells (66).

Transcriptional ren responses to kidney injury

The response of *ren* transcription to kidney injury was assessed by use of a well-characterised acute kidney injury (AKI) model. The aminoglycoside antibiotic gentamicin is toxic to proximal tubular cells (28, 43, 86). Post-injury, adult zebrafish undergo nephron repair followed by *de novo* nephrogenesis to fully restore kidney function by 21 days. The response of whole kidney renin transcription was tested during the injury phase, and during nephron repair and regeneration (43). Renal injury was confirmed two days post injection by a marked upregulation of kidney injury molecule 1 (*kim1*) and a concurrent decrease of the proximal tubular marker *slc201a1*, a sodium-dependent phosphate transporter (Fig. 6*A*-*B*). This was associated with a significant upregulation of *ren* transcription (Fig. 6*I*) implying RAS activation in response to renal injury.

Early markers of nephron progenitors were upregulated during nephron repair and neo-nephrogenesis. Upregulation of *lhx1a* (Fig. 6*E*) eight days post-injury confirmed a reparative response involving activation of renal progenitor cells. There was a trend towards increased transcription of both Wilm's tumor (*wt1*) homologues, but these were not statistically significant (Fig. 6*C*-*D*). *De novo* nephrogenesis is in its early stages eight days post injury and was demonstrated in our study by a maintained low and high transcription of *slc201a1* and *kim1*, respectively. During this early phase of kidney repair, *ren* transcripts returned to normal levels suggesting that the RAS may have a limited function during early kidney repair and neo-nephrogenesis. In the zebrafish mesonephros, renin cells

are not associated with individual new nephrons until the latter stages of neo-nephrogenesis (Fig. 2*L-M*).

The requirement for RAS in renal repair and regeneration was tested using pharmacological RAS inhibition during injury recovery. Expression of *ren* was significantly upregulated as expected with RAS blockade by captopril. Captopril treatment had no marked effect on the resolution of AKI, as determined by the lack of any change in expression of *slc20a1a* and *kim1* transcripts eight days post injury (Fig. 6*F*).

Spatial variation of ren expression

Early nephron progenitor markers are ubiquitously expressed across the head, trunk, and tail regions of the kidney (13). Transcripts *of ren* and *wt1* were determined in the head kidney and compared to the trunk and tail regions. No significant spatial differences were observed in either *wt1* homologues, and both genes were similarly upregulated across the kidney during regeneration (Fig. 7*A-B*). Conversely, *ren*:LifeAct-RFP expression (Fig. 1*D*) and *ren* mRNA transcripts (Fig. 7*C*) were significantly higher in the tail and trunk regions than the head kidney. As previously observed (Fig. 6*F*), *ren* was not significantly upregulated during regeneration.

Discussion

This first study of renin expressing cells in the zebrafish mesonephros reveals two distinct morphologies of renin cell. Only epithelioid-like renin cells contained a secretory intracellular structure consistent with active renin secretion. The *ren*:LifeAct-RFP transgene faithfully recapitulates renin expression in both adult and larval zebrafish (58). As characteristic of the mammalian

mesonephros and developing metanephros (27), zebrafish *ren* is exclusively detected in perivascular cells (19). A low expression of renin mRNA is detectable in the mammalian metanephric proximal tubule (10, 64), but not in zebrafish. The localisation of intrarenal perivascular renin cells in zebrafish is similar to that observed in developing mammals (26, 62). In the human mesonephros (9), and initially the developing mammalian metanephros (9, 26, 62), renin expression is associated with pre-glomerular arteries and arterioles prior to a postnatal restriction to the JGA (20, 22, 26, 47, 62, 73). In the mammalian, and piscine mesonephroi (12, 33), there is no association between renin cells and the distal tubules. Consequently, although present at the pole of the afferent arteriole, mesonephric JG renin cells are not part of a structured JGA.

The lack of granulation in efferent renin cells suggests these post-glomerular perivascular cells differ in their function to their secretory counterparts. In mice, 20-40% of efferent arterioles are renin positive, of which a portion are granulated (73). By virtue of their low cell volume in comparison to the cuboidal secretory renin cells, acidic granules are sparse in their efferent counterparts. Without secretory granules, efferent renin cells are expected to have a limited capacity for the regulated excretion of active renin, but may constitutively secrete pro-renin.

The mesenchymal precursor of the renin-expressing cell is postulated to belong to a pericyte lineage. Mammalian pericytes markers (*Rgs 5*, *NG2* and *CD 146*) are detected in both adult and embryonic renin cells (4, 7, 67, 70). Pericytes and renin cells both derive from mesenchymal *FoxD1* cells (16, 39, 63, 65). Their relationship is evident in experimental renal injury where CoRL repopulate multiple glomerular cell niches, including the mesangium (2, 53-55, 68). The expression of individual pericyte markers in renin cells may be species-specific, since neither adult nor embryonic murine renin cells express *Pdgfrb,* nor do they rely on its expression for their differentiation (49). In larval fish, *pdgfrb*- and *ren*-expressing cells both require Notch signalling for their differentiation and both arise from the lateral mesoderm to occupy the same cell niche at the ventral dorsal aorta (3, 58). As for mammalian

renin cells (49), zebrafish *pdgfrb*-expressing cells do not rely on *pdgfr* signalling for their differentiation (3).

Mammalian renin cells have a reversible phenotype switching from contractile smooth muscle cells to an endocrine renin phenotype during development or physiological challenge (7, 17, 40, 62, 66). In some instances, renin cells of the JGA loose detectable SMA (29, 49, 51). Zebrafish renin cells do not loose SMA expression towards the glomerulus and maintain expression of early pericyte markers. Although the differentiation and phenotypic switch of renin cells may differ across vertebrates, their physiological function appears to be conserved.

Prior to their maturation into JG cells with a full endocrine phenotype (6, 15, 57), embryonic renin cells present at branch points may release paracrine tropic factors required for angiogenesis of nascent renal vessels (56, 58). Experimental ablation of renin cells or RAS during development results in renal vascular defects (21, 39, 77). In the renal vasculature of rats (56), and the anterior mesenteric artery of larval zebrafish (58), renin-expressing cells are associated with branch points. In mice, renin is not preferentially expressed at intrarenal vessel branch points (62). Despite the ubiquitous distribution of nephron progenitors expressing *wt1* across the zebrafish kidney tissue (86), renin cells are lower in density in the head kidney. In our studies of the zebrafish mesonephros, which continually undergoes *de novo* nephrogenesis (86), no angiogenic sprout tips associated with renin cells were observed. In mammals, the RAS may be implicated in angiogenesis via the angiotensin 2 (AT2) receptor-mediated activation of *Vegf*, a potent stimulator of vasculogenesis and angiogenesis (30).

The endocrine phenotype of mesonephric renin cells in zebrafish was confirmed by the presence of either an immature or fully granulated ultrastructure, as characteristic of mammalian renin cells. Embryonic or intermediate mammalian renin cells contain a variable number of small electron dense protogranules (74), as observed in adult zebrafish. Paracrystaline granules, which largely contain prorenin in mammals (72), were also present in the zebrafish renin cells. The numerous uniformly sized electron dense granules characteristic of mature renin cells are also reported in other fish species

(32), and are approximately half the size of mammalian granules. The activation of mammalian renin by the cleavage of pro-renin is proposed to occur due to the acidic milieu of secretory granules (84). The presence of acidic granules suggests that renin activation is likely to be conserved in the zebrafish.

The response of mesonephric renin cells to salinity variation, pharmacological RAS inhibition, and renal injury is consistent with their endocrine function within a functional RAS. With the exception of the MAS receptor, zebrafish contain all components of the RAS including ACE 1 and 2, and both angiotensin (AT) receptors (14). Our data in adult zebrafish showing the modulation of renin mRNA with varying salinity is consistent with a role for the RAS in ion homeostasis, which is also evident in larval zebrafish (25, 34). The robust response of *ren* transcription to tubular injury may be due to tubular obstruction and a reduction in glomerular filtration, or the impaired tubular reabsorption of solutes stimulating tubuloglomerular feedback and associated renin secretion (5, 46). Indeed, the zebrafish gentamicin injury model is known to result in tubular obstruction due to the formation of epithelial casts (24, 44). Impaired solute transport is also expected with a significant decrease in *slc20a1a*-expressing proximal tubular cells.

RAS activity is required for renal development (21, 58, 77), and may be activated during nephron repair and regeneration (78). Eight to nine days post-injury, both tubular repair and *de novo* nephrogenesis occur in the zebrafish (43). Aggregates of nephron progenitor cells expressing *wt1* and *lhx1a* reach a peak by nine days post-injury (13, 86). In our study, upregulation of *lhx1a* confirms the activation of nephron progenitors during repair and regeneration, but this was not associated with an upregulation of *ren.* These data show that although the RAS is activated during renal injury, RAS activity is similar to baseline levels during the initial phase of renal repair.

These data from zebrafish show that, whilst forming two distinct morphological populations, mesonephric renin cells share numerous similarities to their embryonic mammalian counterparts. The characteristic granular and epithelioid renin cell phenotype is maintained in fish. Functionally, mesonephric renin cells respond to RAS-mediated challenges in a similar manner to mammals

demonstrating the conservation of the physiological actions of the RAS across vertebrates. Our studies demonstrate the relevance of adult zebrafish as an excellent model species for evaluating the mechanisms associated with the clinical improvement of renal function under RAS inhibition.

Grants

This work was financially supported by a British Heart Foundation Centre of Research Excellence award and Kidney Research UK. The authors also acknowledge financial support from the Wellcome Trust for the zebrafish facility.

Acknowledgements

The authors thank Prof. K. Kawakami, Prof. D. Lyons, and Dr. T. Czopka for Tol2 kit plasmids; Prof. Didier Stainier for the *acta2:*GFP line; Prof. B. Peault, Dr Charlotte Buckley and Dr. C. Tucker for helpful discussions; and facility staff for fish husbandry.

Disclosures

None

References

1. **Abel MH, Charlton HM, Huhtaniemi I, Pakarinen P, Kumar TR, and Christian HC**. An investigation into pituitary gonadotrophic hormone synthesis, secretion, subunit gene expression and cell structure in normal and mutant male mice. *J Neuroendocrinol* 25: 863-875, 2013.
2. **Altintas MM, and Reiser J**. Bridges to cross, burn, and mend: cells of renin lineage as podocyte progenitors. In: *American journal of physiology Renal physiology*. United States: 2015, p. F499-500.
3. **Ando K, Fukuhara S, Izumi N, Nakajima H, Fukui H, Kelsh RN, and Mochizuki N**. Clarification of mural cell coverage of vascular endothelial cells by live imaging of zebrafish. *Development* 143: 1328-1339, 2016.

4. **Armulik A, Genove G, and Betsholtz C**. Pericytes: developmental, physiological, and pathological perspectives, problems, and promises. *Dev Cell* 21: 193-215, 2011.
5. **Basile DP, Anderson MD, and Sutton TA**. Pathophysiology of Acute Kidney Injury. *Comprehensive Physiology* 2: 1303-1353, 2012.
6. **Bergers G, and Song S**. The role of pericytes in blood-vessel formation and maintenance. *Neuro-oncology* 7: 452-464, 2005.
7. **Brunskill EW, Sequeira-Lopez MLS, Pentz ES, Lin E, Yu J, Aronow BJ, Potter SS, and Gomez RA**. Genes that Confer the Identity of the Renin Cell. *Journal of the American Society of Nephrology* 22: 2213-2225, 2011.
8. **Capréol SV, and Sutherland LE**. Comparative morphology of juxtaglomerular cells. I. Juxtaglomerular cells in fish. *Canadian Journal of Zoology* 46: 249-256, 1968.
9. **Celio MR, Groscurth P, and Inagami T**. Ontogeny of renin immunoreactive cells in the human kidney. *Anat Embryol (Berl)* 173: 149-155, 1985.
10. **Chen M, Harris MP, Rose D, Smart A, He XR, Kretzler M, Briggs JP, and Schnermann J**. Renin and renin mRNA in proximal tubules of the rat kidney. *Journal of Clinical Investigation* 94: 237-243, 1994.
11. **Choi J, Dong L, Ahn J, Dao D, Hammerschmidt M, and Chen J-N**. FoxH1 negatively modulates flk1 gene expression and vascular formation in zebrafish. *Developmental Biology* 304: 735-744, 2007.
12. **de Martino C, and Zamboni L**. A morphologic study of the mesonephros of the human embryo. *Journal of ultrastructure research* 16: 399-427, 1966.
13. **Diep CQ, Ma D, Deo RC, Holm TM, Naylor RW, Arora N, Wingert RA, Bollig F, Djordjevic G, Lichman B, Zhu H, Ikenaga T, Ono F, Englert C, Cowan CA, Hukriede NA, Handin RI, and Davidson AJ**. Identification of adult nephron progenitors capable of kidney regeneration in zebrafish. *Nature* 470: 95-100, 2011.
14. **Fournier D, Luft FC, Bader M, Ganten D, and Andrade-Navarro MA**. Emergence and evolution of the renin-angiotensin-aldosterone system. *Journal of Molecular Medicine-Jmm* 90: 495-508, 2012.
15. **Gaengel K, Genove G, Armulik A, and Betsholtz C**. Endothelial-mural cell signaling in vascular development and angiogenesis. *Arteriosclerosis, thrombosis, and vascular biology* 29: 630-638, 2009.
16. **Gomez IG, and Duffield JS**. The FOXD1 lineage of kidney perivascular cells and myofibroblasts: functions and responses to injury. *Kidney international supplements* 4: 26-33, 2014.
17. **Gomez RA, Belyea B, Medrano S, Pentz ES, and Sequeira-Lopez MLS**. Fate and plasticity of renin precursors in development and disease. *Pediatric Nephrology* 29: 721-726, 2014.
18. **Gomez RA, Lynch KR, Chevalier RL, Everett AD, Johns DW, Wilfong N, Peach MJ, and Carey RM**. Renin and angiotensinogen gene expression and intrarenal renin distribution during ACE inhibition. *Am J Physiol* 254: F900-906, 1988.
19. **Gomez RA, Lynch KR, Sturgill BC, Elwood JP, Chevalier RL, Carey RM, and Peach MJ**. Distribution of renin mRNA and its protein in the developing kidney. *Am J Physiol* 257: F850-858, 1989.
20. **Gomez RA, Pupilli C, and Everett AD**. Molecular and cellular aspects of renin during kidney ontogeny. *Pediatric Nephrology* 5: 80-87, 1991.
21. **Guron G, and Friberg P**. An intact renin-angiotensin system is a prerequisite for normal renal development. *Journal of hypertension* 18: 123-137, 2000.
22. **Hackenthal E, Paul M, Ganten D, and Taugner R**. Morphology, physiology, and molecular-biology of renin secretion. *Physiological Reviews* 70: 1067-1116, 1990.
23. **Harding P, Sigmon DH, Alfie ME, Huang PL, Fishman MC, Beierwaltes WH, and Carretero OA**. Cyclooxygenase-2 mediates increased renal renin content induced by low-sodium diet. *Hypertension* 29: 297-302, 1997.

24. **Hentschel DM, Park KM, Cilenti L, Zervos AS, Drummond I, and Bonventre JV**. Acute renal failure in zebrafish: a novel system to study a complex disease. *American journal of physiology Renal physiology* 288: F923-929, 2005.
25. **Hoshijima K, and Hirose S**. Expression of endocrine genes in zebrafish larvae in response to environmental salinity. *Journal of Endocrinology* 193: 481-491, 2007.
26. **Jones CA, Hurley MI, Black TA, Kane CM, Pan L, Pruitt SC, and Gross KW**. Expression of a renin/GFP transgene in mouse embryonic, extra-embryonic, and adult tissues. *Physiological Genomics* 4: 75-81, 2000.
27. **Jones CA, Sigmund CD, McGowan RA, Kanehaas CM, and Gross KW**. Expression of murine renin genes during fetal development. *Molecular Endocrinology* 4: 375-383, 1990.
28. **Kamei CN, Liu Y, and Drummond IA**. Kidney Regeneration in Adult Zebrafish by Gentamicin Induced Injury. *Journal of visualized experiments : JoVE* e51912, 2015.
29. **Karger C, Kurtz F, Steppan D, Schwarzensteiner I, Machura K, Angel P, Banas B, Risteli J, and Kurtz A**. Procollagen I-expressing renin cell precursors. *American journal of physiology Renal physiology* 305: F355-361, 2013.
30. **Khakoo AY, Sidman RL, Pasqualini R, and Arap W**. Does the renin-angiotensin system participate in regulation of human vasculogenesis and angiogenesis? *Cancer research* 68: 9112-9115, 2008.
31. **Kobori H, Nangaku M, Navar LG, and Nishiyama A**. The intrarenal renin-angiotensin system: from physiology to the pathobiology of hypertension and kidney disease. *Pharmacological reviews* 59: 251-287, 2007.
32. **Kon Y, Hashimoto Y, Kitagawa H, and Kudo N**. Morphological and immunohistochemical studies of juxtaglomerular cells in the carp, Cyprinus carpio. *Nihon juigaku zasshi The Japanese journal of veterinary science* 49: 323-331, 1987.
33. **Krishnamurthy VG, and Bern HA**. Correlative histologic study of the corpuscles of Stannius and the juxtaglomerular cells of teleost fishes. *General and Comparative Endocrinology* 13: 313-335, 1969.
34. **Kumai Y, Bernier NJ, and Perry SF**. Angiotensin-II promotes Na+ uptake in larval zebrafish, Danio rerio, in acidic and ion-poor water. *Journal of Endocrinology* 220: 195-205, 2014.
35. **Kurt B, and Kurtz A**. Plasticity of renal endocrine function. *American journal of physiology Regulatory, integrative and comparative physiology* 308: R455-466, 2015.
36. **Kurtz A**. Renin Release: Sites, Mechanisms, and Control. *Annual Review of Physiology, Vol 73* 73: 377-399, 2011.
37. **Kwan KM, Fujimoto E, Grabher C, Mangum BD, Hardy ME, Campbell DS, Parant JM, Yost HJ, Kanki JP, and Chien C-B**. The Tol2kit: A multisite Gateway-based construction kit for Tol2 transposon transgenesis constructs. *Developmental Dynamics* 236: 3088-3099, 2007.
38. **Liang P, Jones CA, Bisgrove BW, Song L, Glenn ST, Yost HJ, and Gross KW**. Genomic characterization and expression analysis of the first nonmammalian renin genes from zebrafish and pufferfish. *Physiological Genomics* 16: 314-322, 2004.
39. **Lin EE, Sequeira-Lopez MLS, and Gomez RA**. RBP-J in FOXD1+renal stromal progenitors is crucial for the proper development and assembly of the kidney vasculature and glomerular mesangial cells. *American Journal of Physiology-Renal Physiology* 306: F249-F258, 2014.
40. **Lopez M, Pentz ES, Robert B, Abrahamson DR, and Gomez RA**. Embryonic origin and lineage of juxtaglomerular cells. *American Journal of Physiology-Renal Physiology* 281: F345-F356, 2001.
41. **Lopez ML, and Gomez RA**. The renin phenotype: roles and regulation in the kidney. *Current opinion in nephrology and hypertension* 19: 366-371, 2010.
42. **Lumbers ER**. Functions of the renin-angiotensin system during development. *Clin Exp Pharmacol Physiol* 22: 499-505, 1995.
43. **McCampbell KK, Springer KN, and Wingert RA**. Atlas of Cellular Dynamics during Zebrafish Adult Kidney Regeneration. *Stem Cells Int* 2015: 547636, 2015.

44. **McKee RA, and Wingert RA**. Zebrafish Renal Pathology: Emerging Models of Acute Kidney Injury. *Current Pathobiology Reports* 3: 171-181, 2015.
45. **Methot D, and Reudelhuber TL**. Knockout of renin-angiotensin system genes: effects on vascular development. *Current hypertension reports* 3: 68-73, 2001.
46. **Metzger R, Bohle RM, Pauls K, Eichner G, Alhenc-Gelas F, Danilov SM, and Franke FE**. Angiotensin-converting enzyme in non-neoplastic kidney diseases. *Kidney Int* 56: 1442-1454, 1999.
47. **Minuth M, Hackenthal E, Poulsen K, Rix E, and Taugner R**. Renin immunocytochemistry of the differentiating juxtaglomerular apparatus. *Anatomy and Embryology* 162: 173-181, 1981.
48. **Neubauer B, Machura K, Chen M, Weinstein LS, Oppermann M, Sequeira-Lopez ML, Gomez RA, Schnermann J, Castrop H, Kurtz A, and Wagner C**. Development of vascular renin expression in the kidney critically depends on the cyclic AMP pathway. *American journal of physiology Renal physiology* 296: F1006-1012, 2009.
49. **Neubauer B, Machura K, Rupp V, Tallquist MD, Betsholtz C, Sequeira-Lopez ML, Ariel Gomez R, and Wagner C**. Development of renal renin-expressing cells does not involve PDGF-B-PDGFR-beta signaling. *Physiological reports* 1: e00132, 2013.
50. **Nishimura H, and Ogawa M**. The Renin-Angiotensin System in Fishes. *American Zoologist* 13: 823-838, 1973.
51. **Park S, and Harrison-Bernard LM**. Augmented Renal Vascular nNOS and Renin Protein Expression in Angiotensin Type 1 Receptor Null Mice. *Journal of Histochemistry and Cytochemistry* 56: 401-414, 2008.
52. **Perner B, Englert C, and Bollig F**. The Wilms tumor genes wt1a and wt1b control different steps during formation of the zebrafish pronephros. *Developmental Biology* 309: 87-96, 2007.
53. **Pippin JW, Glenn ST, Krofft RD, Rusiniak ME, Alpers CE, Hudkins K, Duffield JS, Gross KW, and Shankland SJ**. Cells of renin lineage take on a podocyte phenotype in aging nephropathy. *American journal of physiology Renal physiology* 306: F1198-1209, 2014.
54. **Pippin JW, Kaverina NV, Eng DG, Krofft RD, Glenn ST, Duffield JS, Gross KW, and Shankland SJ**. Cells of renin lineage are adult pluripotent progenitors in experimental glomerular disease. *Am J Physiol Renal Physiol* 309: F341-358, 2015.
55. **Pippin JW, Sparks MA, Glenn ST, Buitrago S, Coffman TM, Duffield JS, Gross KW, and Shankland SJ**. Cells of renin lineage are progenitors of podocytes and parietal epithelial cells in experimental glomerular disease. *The American journal of pathology* 183: 542-557, 2013.
56. **Reddi V, Zaglul A, Pentz ES, and Gomez RA**. Renin-expressing cells are associated with branching of the developing kidney vasculature. *Journal of the American Society of Nephrology* 9: 63-71, 1998.
57. **Ribatti D, Nico B, and Crivellato E**. The role of pericytes in angiogenesis. *The International journal of developmental biology* 55: 261-268, 2011.
58. **Rider SA, Mullins LJ, Verdon RF, MacRae CA, and Mullins JJ**. Renin expression in developing zebrafish is associated with angiogenesis and requires the Notch pathway and endothelium. *American journal of physiology Renal physiology* ajprenal.00247.02015, 2015.
59. **Rider SA, Tucker CS, del-Pozo J, Rose KN, MacRae CA, Bailey MA, and Mullins JJ**. Techniques for the in vivo assessment of cardio-renal function in zebrafish (Danio rerio) larvae. *Journal of Physiology-London* 590: 1803-1809, 2012.
60. **Riedl J, Crevenna AH, Kessenbrock K, Yu JH, Neukirchen D, Bista M, Bradke F, Jenne D, Holak TA, Werb Z, Sixt M, and Wedlich-Soldner R**. Lifeact: a versatile marker to visualize F-actin. *Nature methods* 5: 605-607, 2008.
61. **Romagnani P, Lasagni L, and Remuzzi G**. Renal progenitors: an evolutionary conserved strategy for kidney regeneration. *Nature reviews Nephrology* 9: 137-146, 2013.
62. **Sauter A, Machura K, Neubauer B, Kurtz A, and Wagner C**. Development of renin expression in the mouse kidney. *Kidney International* 73: 43-51, 2008.

63. **Sequeira-Lopez ML, Lin EE, Li M, Hu Y, Sigmund CD, and Gomez RA**. The earliest metanephric arteriolar progenitors and their role in kidney vascular development. *American journal of physiology Regulatory, integrative and comparative physiology* 308: R138-149, 2015.
64. **Sequeira-Lopez ML, Nagalakshmi VK, Li M, Sigmund CD, and Gomez RA**. Vascular versus tubular renin: role in kidney development. *American journal of physiology Regulatory, integrative and comparative physiology* ajpregu.00313.02015, 2015.
65. **Sequeira Lopez ML, and Gomez RA**. Development of the renal arterioles. *J Am Soc Nephrol* 22: 2156-2165, 2011.
66. **Sequeira Lopez MLS, Pentz ES, Nomasa T, Smithies O, and Gomez RA**. Renin cells are precursors for multiple cell types that switch to the renin phenotype when homeostasis is threatened. *Developmental cell* 6: 719-728, 2004.
67. **Smith SW, Chand S, and Savage CO**. Biology of the renal pericyte. In: *Nephrology, dialysis, transplantation : official publication of the European Dialysis and Transplant Association - European Renal Association*. England: 2012, p. 2149-2155.
68. **Starke C, Betz H, Hickmann L, Lachmann P, Neubauer B, Kopp JB, Sequeira-Lopez ML, Gomez RA, Hohenstein B, Todorov VT, and Hugo CP**. Renin lineage cells repopulate the glomerular mesangium after injury. *J Am Soc Nephrol* 26: 48-54, 2015.
69. **Stefanska A, Kenyon C, Christian HC, Buckley C, Shaw I, Mullins JJ, and Peault B**. Human kidney pericytes produce renin. *Kidney Int* In Press: 2016.
70. **Stefanska A, Peault B, and Mullins JJ**. Renal pericytes: multifunctional cells of the kidneys. *Pflugers Archiv : European journal of physiology* 465: 767-773, 2013.
71. **Steppan D, Zügner A, Rachel R, and Kurtz A**. Structural analysis suggests that renin is released by compound exocytosis. *Kidney Int* 83: 233-241, 2013.
72. **Tangner R, Murakami K, and Kim SJ**. Renin activation in juvenile secretory granules? *Histochemistry* 85: 107-109, 1986.
73. **Taugner R, and Hackenthal E**. Morphology of the Juxtaglomerular Apparatus. In: *The Juxtaglomerular Apparatus: Structure and Function*, edited by Taugner R, and Hackenthal E. Berlin, Heidelberg: Springer Berlin Heidelberg, 1989, p. 5-43.
74. **Taugner R, and Hackenthal E**. Synthesis and Traffic of Renin in Epithelioid Cells. In: *The Juxtaglomerular Apparatus: Structure and Function*, edited by Taugner R, and Hackenthal E. Berlin, Heidelberg: Springer Berlin Heidelberg, 1989, p. 103-126.
75. **Thisse C, and Thisse B**. High-resolution in situ hybridization to whole-mount zebrafish embryos. In: *Nat Protoc*. England: 2008, p. 59-69.
76. **Tikellis C, Bernardi S, and Burns WC**. Angiotensin-converting enzyme 2 is a key modulator of the renin-angiotensin system in cardiovascular and renal disease. *Current opinion in nephrology and hypertension* 20: 62-68, 2011.
77. **Tufro-McReddie A, Romano LM, Harris JM, Ferder L, and Gomez RA**. Angiotensin II regulates nephrogenesis and renal vascular development. *Am J Physiol* 269: F110-115, 1995.
78. **van der Meer IM, Cravedi P, and Remuzzi G**. The role of renin angiotensin system inhibition in kidney repair. *Fibrogenesis & tissue repair* 3: 7, 2010.
79. **Wang Y, Pan L, Moens CB, and Appel B**. Notch3 establishes brain vascular integrity by regulating pericyte number. *Development* 141: 307-317, 2014.
80. **Westerfield M**. *The Zebrafish Book. A Guide for the Laboratory Use of Zebrafish (Brachydanio rerio)* Eugene, OR. : University of Oregon Press, 1995.
81. **White RM, Sessa A, Burke C, Bowman T, LeBlanc J, Ceol C, Bourque C, Dovey M, Goessling W, Burns CE, and Zon LI**. Transparent adult zebrafish as a tool for in vivo transplantation analysis. *Cell Stem Cell* 2: 183-189, 2008.
82. **Whitesell TR, Kennedy RM, Carter AD, Rollins E-L, Georgijevic S, Santoro MM, and Childs SJ**. An alpha-Smooth Muscle Actin (acta2/alpha sma) Zebrafish Transgenic Line Marking Vascular Mural Cells and Visceral Smooth Muscle Cells. *Plos One* 9: 2014.

83. **Wiens KM, Lee HL, Shimada H, Metcalf AE, Chao MY, and Lien CL**. Platelet-derived growth factor receptor beta is critical for zebrafish intersegmental vessel formation. *PLoS One* 5: e11324, 2010.
84. **Xa LK, Lacombe MJ, Mercure C, Lazure C, and Reudelhuber TL**. General lysosomal hydrolysis can process prorenin accurately. *American journal of physiology Regulatory, integrative and comparative physiology* 307: R505-513, 2014.
85. **Yang TX, Endo Y, Huang YG, Smart A, Briggs JP, and Schnermann J**. Renin expression in COX-2-knockout mice on normal or low-salt diets. *American Journal of Physiology-Renal Physiology* 279: F819-F825, 2000.
86. **Zhou W, Boucher RC, Bollig F, Englert C, and Hildebrandt F**. Characterization of mesonephric development and regeneration using transgenic zebrafish. *American journal of physiology Renal physiology* 299: F1040-1047, 2010.

Figure Legends

Figure 1. Distribution and morphology of mesonephric renin cells. *A*: The location and morphology of mesonephric renin cells was assessed across the whole kidney by *in situ* hybridisation and tg(*ren*:LifeAct-RFP, *kdrl*:EGFP). *A-C*: *In situ* hybridisations with background structures stained by methyl green and *ren* mRNA detected by NBT (blue). Perivascular *ren* is associated with intrarenal vessels (*A-B*) and not detected in proximal (†) or distal tubules (*), nor inside glomeruli (dashed outline). Scale bars 20 μm. GFP and RFP fluorescently label endothelial and renin cells, respectively. *D*: Ventral view of the whole adult kidney in tg(*ren*:LifeAct-RFP) showing prominent and sparse expression of *ren*:LifeAct-RFP in the trunk and tail regions compared to the head kidney, respectively. *E-G*: Maximum intensity projections of tg(*ren*:LifeAct-RFP, *kdrl*:EGFP). *E*: Group of glomeruli and associated vasculature showing *ren*:LifeAct-RFP at the afferent arterioles (white ovals) and weaker *ren*:LifeAct-RFP at the efferent arterioles (white arrows). A larger pre-glomerular artery is indicated by the yellow arrow. Scale bar 50 μm. *F*: Expression of *ren*:LifeAct-RFP at pre-glomerular arteries. The white arrow shows a branch to an efferent arteriole with *ren*:LifeAct-RFP and the asterisk shows a branch without *ren*:LifeAct-RFP. *G*: Juxtaglomerular (JG) *ren*:LifeAct-RFP at the afferent arteriole. Scale bars 25 μm. *H*: Schematic showing localization of renin cells (red) in the renal vasculature (green); renal artery (*RA*), pre-glomerular artery (*PGA*), afferent arteriole (*AA*), efferent arteriole (*EA*). *I-J*: Single 1 μm optical sections of tg(*ren*:LifeAct-RFP, *kdrl*:EGFP). *I*: Cross

section of multi-cell epithelioid renin cluster at a pre-glomerular artery. Boundaries of cuboidal shaped renin cells are demarcated by *ren*:LifeAct-RFP. *J*: Cross section of an efferent arteriole showing the thin and small cell body (arrow) of an efferent perivascular renin-expressing cell. Scale bars 10 µm. *K*: Schematic showing the cross sections of (1) JG and pre-glomerular renin cell clusters (red arrows) with intermediate smooth muscle cells (green arrow), and (2) efferent arteriolar renin cells. JG and pre-glomerular renin cells are present as multicellular clusters. Efferent renin cells surround the endothelium with thin-bodied cells that have a low cytoplasmic volume.

Figure 2. Expression of smooth muscle and pericyte markers in mesonephric renin cells. To determine the relationship of renin-expressing cells with smooth muscle cells and pericytes, *ren*:LifeAct-RFP fish were crossed to transgenic lines for established mural cell markers. In mammals and fish, *Pdgfrβ* is an early marker of pericytes and smooth muscle actin (*Acta2*) is a marker of mature pericytes and smooth muscle cells. Expression of perivascular cell markers was assessed in JG, pre-glomerular and efferent *ren*:LifeAct-RFP expressing cells. *A*: Maximum intensity projection of tg(*ren*:LifeAct-RFP, *acta2*:EGFP) shows co-expression of *acta2*-EGFP and *ren*:LifeAct-RFP in the juxtaglomerular (JG) afferent and efferent cells (glomerulus white outline, efferent arteriole white arrow, afferent arteriole yellow arrow). Scale bar 50 µm. *B-E*: Single 0.5 µm optical sections of tg(*ren*:LifeAct-RFP, *acta2*:EGFP). *B:* Shows JG renin cell clusters strongly express *acta2*. Circular filamentous actin are highest in density at the luminal region of renin expressing cells. Scale bar 50 µm. *C*: Both *acta2*-EGFP and *ren*:LifeAct-RFP are also co-expressed in pre-glomerular arteriolar renin clusters (white arrows) in tg(*ren*:LifeAct-RFP, *acta2*:EGFP). Scale bar 25 µm. *D:* Clusters of *ren*:LifeAct-RFP express *acta2*-EGFP at a pre-glomerular branch point in tg(*ren*:LifeAct-RFP, *acta2*:EGFP). Scale bar 25 µm. *E*: Detail of pre-glomerular arteriolar cells from plate D showing renin cells have a cuboidal shape in contrast to neighbouring and thinner-bodied smooth muscle cells (white arrow). Scale bar 10 µm. *F*: Expression of *acta2*:EGFP is always present but variable as shown by the projection of weaker expression in some pre-glomerular renin cell clusters. Scale bar 25 µm. *G-H*: 0.5 µm optical sections of tg(*ren*:LifeAct-RFP, *pdgfrβ*:EGFP) showing detail of *pdgfrβ*-EGFP

expression at both a pre-glomerular artery (*G*), and in JG cells (*H*). Scale bars 10 µm. *I*: A single 0.5 µm optical section of tg(*ren*:LifeAct-RFP, *pdgfrβ*:EGFP) showing co-expression of *ren*:LifeAct-RFP and *pdgfrβ*-EGFP in the afferent JG cells (yellow arrow). The efferent arteriole (white arrow) also expresses *pdgfrβ*-EGFP; glomerulus white outline. Scale bar 25 µm. *J*-K: Confocal projections of nuclei stained with DAPI (grey) inside *ren*:LifeAct-RFP -expressing cells (yellow outlines) confirm the multi-cellular structure of renin cell clusters (*J*). In renin cells of the efferent arterioles, nuclei are flattened occupying a thin-bodied cell (*K*). Nuclei not outlined within *ren*:LifeAct-RFP regions are endothelial. Scale bars 10 µm. *L*-*M*: Tg (*ren*:LifeAct-RFP, *wt1b*:GFP) showing early- (*L*) and late-stage(*M*) nascent nephron clusters expressing Wilm's tumor (*wt1b:*GFP). Expression of *ren*:LifeAct-RFP is only detected in the latter stages of nephron development and is associated with the juxtaglomerular cells of the afferent arteriole. Glomeruli (*). Scale bars 25µm.

Figure 3. Presence of acidic intracellular vesicles in renin cells. To test for the presence of acidic granules in individual cells across the mesonephric kidney, whole kidney squashes of tg(*ren*:LifeAct-RFP) were stained with lysotracker green. Single 0.5 µm optical sections were taken by confocal microscopy to assess staining in *ren*:LifeAct-RFP expressing cells. *A*: A juxtaglomerular *ren*-RFP cell cluster with regions of punctate intracellular lysotracker staining (white arrows). *B*: Pre-glomerular arteriolar renin cell cluster also with regions of punctate lysotracker staining (white arrows). *C*: Efferent arteriole showing very occasional lysotracker stained vesicles (arrows). All Scale bars 10 µm.

Figure 4. Intracellular ultrastructure of mesonephric renin cells. The intracellular structure of renin expressing cells was determined by electron microscopy. Renin expressing cells in tg(*ren*:LifeAct-RFP) were identified using 15 nm immunogold labelling against *ren*:LifeAct-RFP. Example immunogold particles are highlighted with black arrows and mitochondria with 'M'. Immunogold staining is specific, only being present in the cytoplasm and not nuclei. *A*: Gold-labelled *ren*:LifeAct-RFP cell with a highly vacuolated intracellular structure and several mitochondria. The rectangle outline is of plate *B*. Scale bar 2 µm. *B*: A higher magnification of plate *A* shows detail of clear vesicles, some of

which are partially filled with electron dense material (white arrows). Scale bar 400 nm. *C & D*: Immunogold labelled cells with a vacuolated intracellular structure and occasional 50-200 nm electron dense granules with paracrystaline content (white arrows). Insert in *C* shows detail of highlighted (white arrow) paracrystaline granules in *C*. Scale bars (*C*) 200 and (*D*) 500 nm. *E*: Standard EM showing renin and endothelial cells, the latter recognisable by elongated nuclei. The vessel lumen is visible (L). Rectangle outline is of plate *G*. Scale bar 2µm. *F & G*: Higher magnification of *E* showing numerous 150-400 nm electron dense granules. Scale bars (*F* & *G*) 1 µm. *H*: Intracellular structure of immunogold labelled cell showing electron dense granules of similar size (150-350 nm). Scale bar 1 µm.

Figure 5. Transcriptional response of whole kidney *ren to* salinity and captopril. To determine if variation in salinity *initiated* a homeostatic response, adult fish were exposed to varying ambient salinities. *A*: The 24 hr exposure to varied salinity decreased *ren* expression with increasing salinity and vice versa. *B*: The upregulation of *ren* due the lack of a negative feedback on transcription associated with RAS inhibition was determined in fish treated with 0.5 mM waterborne captopril for four days. This resulted in a significant upregulation of renin mRNA.

Figure 6. Effect of renal damage on renin expression and effect of RAS inhibition on kidney regeneration. To test responses of *ren* transcription to renal injury and regeneration, mRNA expression was tested in whole kidney. The role for RAS during regeneration was tested using captopril RAS inhibition from 24 hrs post injection. Renal damage was induced by 65 mg kg^{-1} I.P. gentamicin injection and analysed at two days post injection (dpi). Whole kidneys were analysed both with and without 0.5 mM waterborne captopril during kidney regeneration at eight dpi. *A*: The decrease of the proximal tubular marker, solute carrier *slc20a1a,* confirms damage of the proximal tubule at both two and eight dpi. *B*: Kidney damage is also confirmed by the upregulation of kidney injury molecule *(kim1*) at two and eight dpi. *C & D:* The slight increase of both *Wilm's tumor* homologues is not significant at 8 dpi. *Wilm's tumor 1b is* upregulated in regenerating kidneys

subject to captopril treatment. *E*: The nephron progenitor marker *LIM homeobox 1a* (*lhx1a*) is upregulated eight days post injection confirming a regenerative response. Expression of *lhx1a is* not affected by captopril treatment. *F*: Renin mRNA is upregulated with the renal injury at two dpi. Expression of *ren* subsequently decreases to control levels after the renal tissue progresses from an injury phase to regeneration at eight dpi. As occurs under normal conditions, renin expression is increased by captopril in regenerating kidneys.

Figure 7. Effect of kidney regeneration on *ren* expression in head kidney versus tail and trunk regions. To determine any involvement of renin in kidney regeneration, *ren* mRNA was assessed in separate regions of the regenerating kidney. Differences in mRNA transcripts were tested between the head kidney and trunk and tail region. Regenerating kidneys were selected based on the up regulation of the nephron progenitor marker, Wilm's tumor. Renal damage and the subsequent regenerative response was induced by 75 mg kg^{-1} I.P. injected gentamicin. Expression of mRNA was analysed at nine days post injection (dpi). *A*-*B*: Both homologues of the Wilm's tumor, are increased at nine dpi but differences between regions are not significant. *C*: The tail and trunk kidney region has significantly more *ren* mRNA than the head kidney. Slight increases in *ren* mRNA with regeneration were not significant at nine dpi.

Table

Gene	Forward	Reverse	UPL probe
rps18	GATGGGAAATACAGCCAGGTC	CCAGAAGTGACGGAGACCAC	41
eef1a1l1 (ef1a)	CCTTCGTCCCAATTTCAGG	CCTTGAACCAGCCCATGTT	67
ren	AGGCAAGTGGGAGGTCATC	CCATCCTTGCAAAACAGGAT	43
wt1a	TTACCTGTCCAACTGCATGG	GCGTGTGGCCATAGTTTGA	1
wt1b	GGCCTGGAATCCTGTTAGC	CAGAGGAGGTGCTCCTGAAG	107
slc201a1	GACTCCCAGTCAGCACTACTCA	CGGAAAAGATGCCAATCG	36

havcr1 (kim1)	AAACCAGAGCCTCGCTAGAA	CCACAGCCATCTCTCTGTTGT	74
lhx1a	AGTCCGAGAAGAATGCGAAC	GGCCGTAGTACTCGCTTTGA	80

Table 1. Primer sequences and Roche UPL probe number for q-PCR analysis.

Figure 1

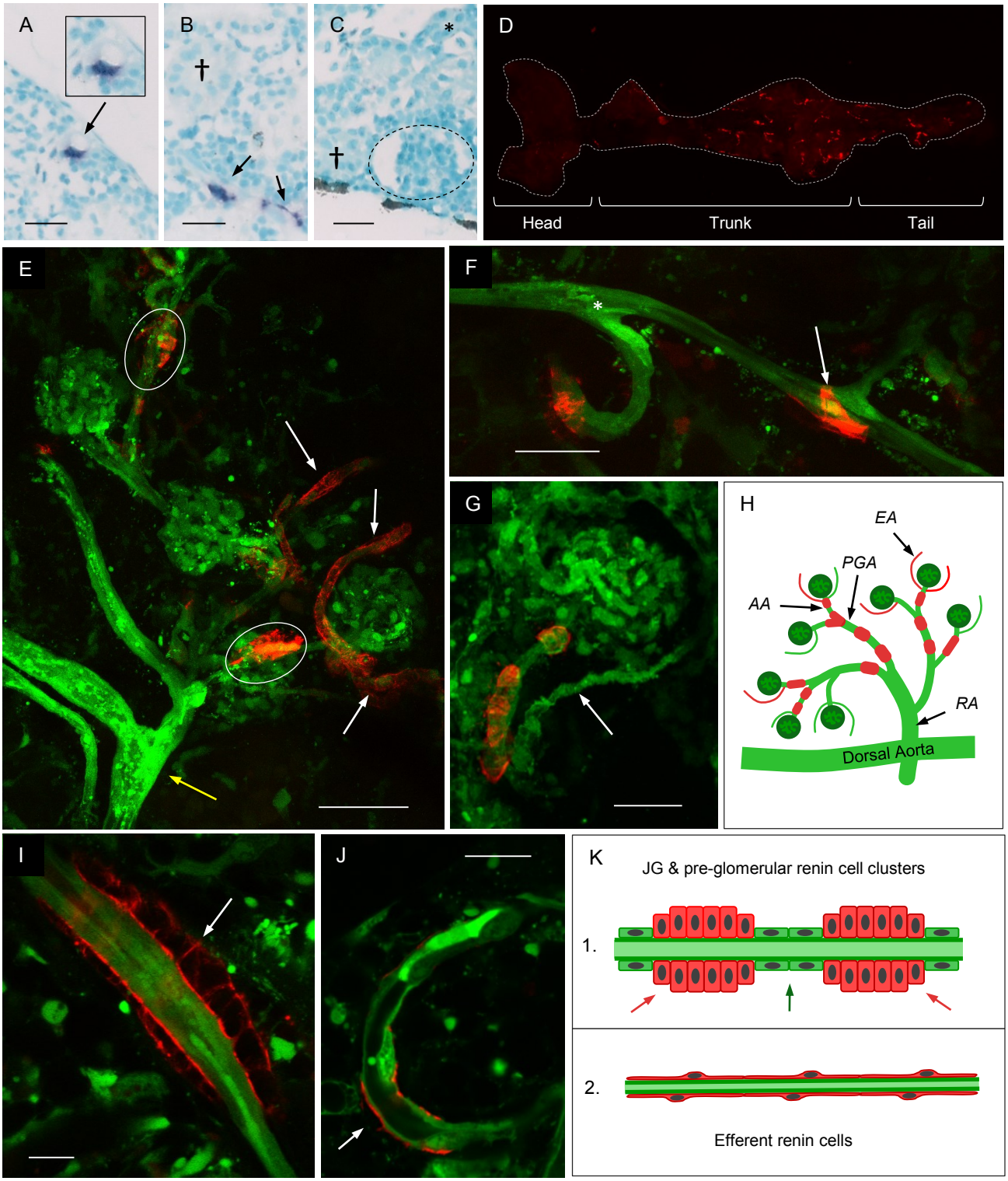
A
B
C
D
Head
Trunk
Tail
E
F
G
H
EA
PGA
AA
RA
Dorsal Aorta
I
J
K
JG & pre-glomerular renin cell clusters
1.
2.
Efferent renin cells

Figure 2

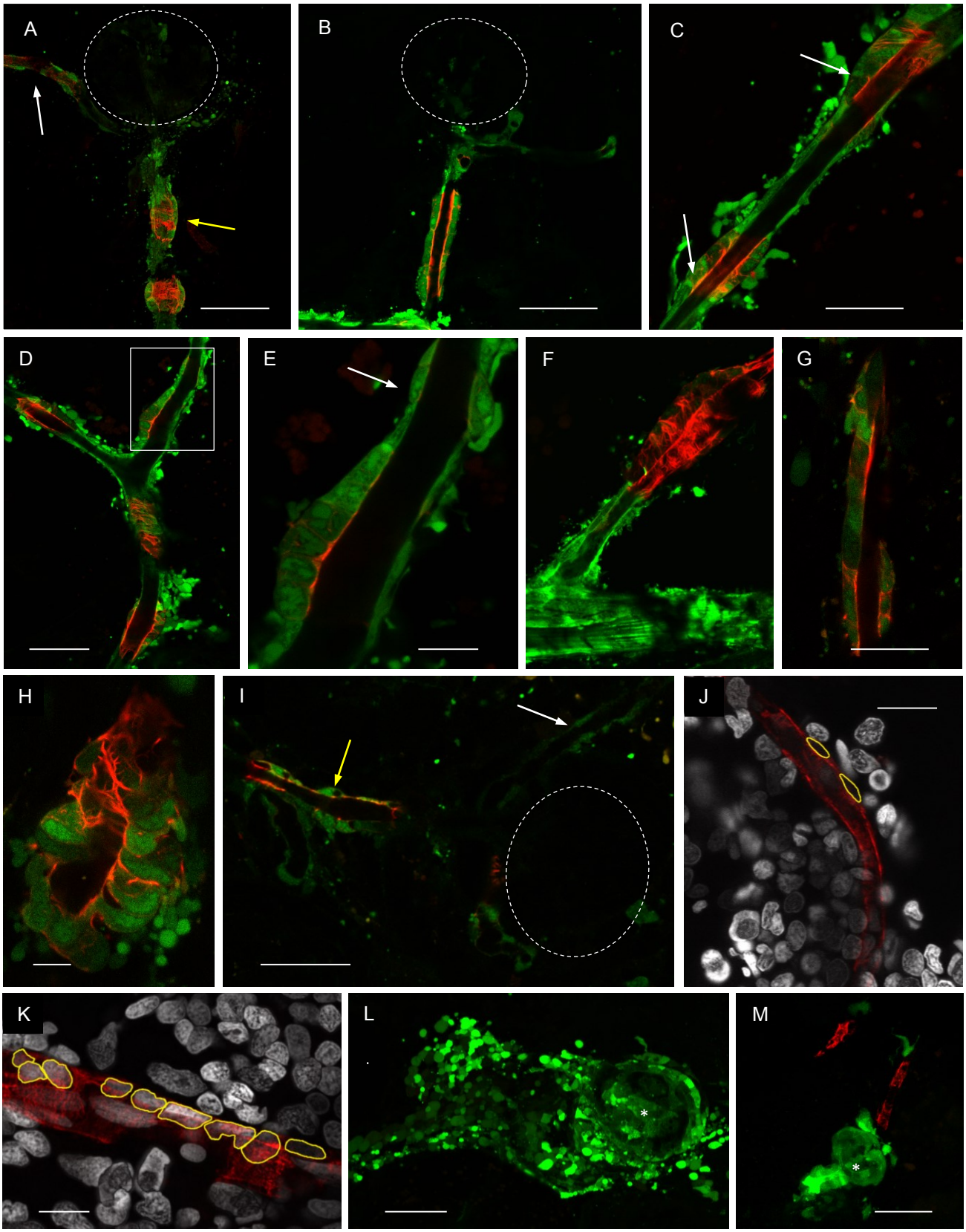

Figure 3

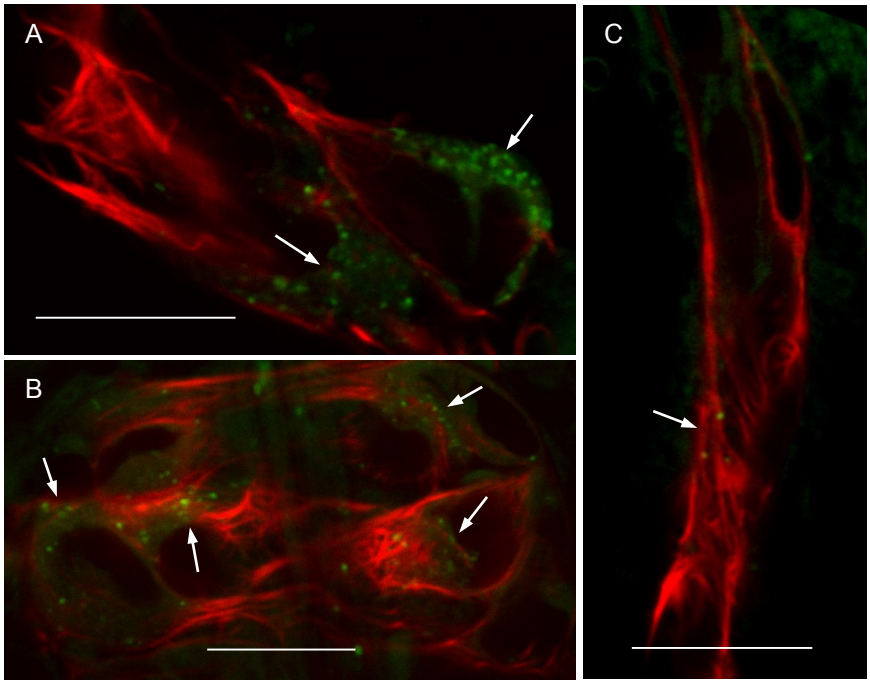

Figure 4

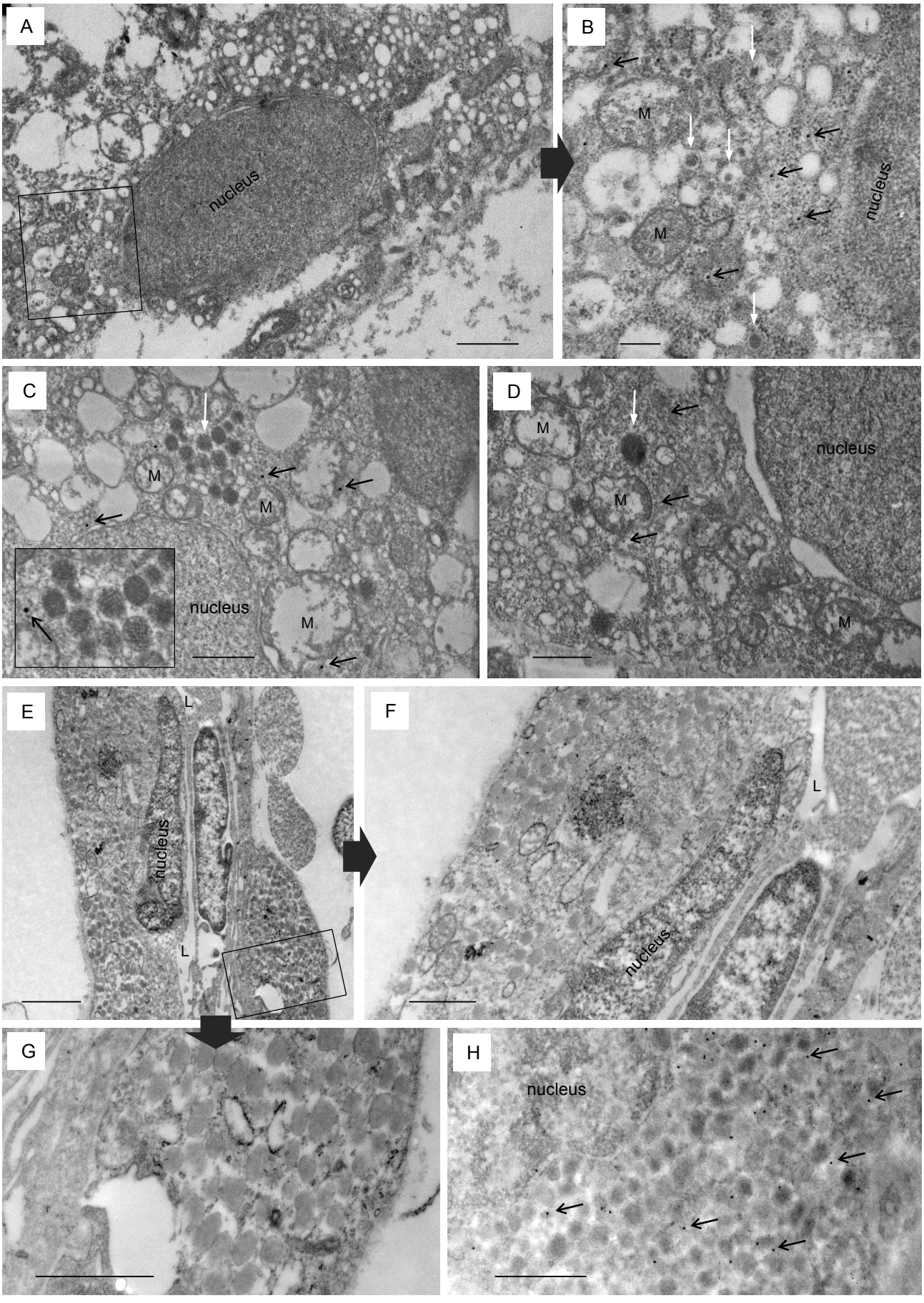
A
nucleus
B
M
M
nucleus
C
M
M
nucleus
M
D
M
nucleus
M
M
E
L
nucleus
L
F
L
nucleus
G
H
nucleus

Figure 5

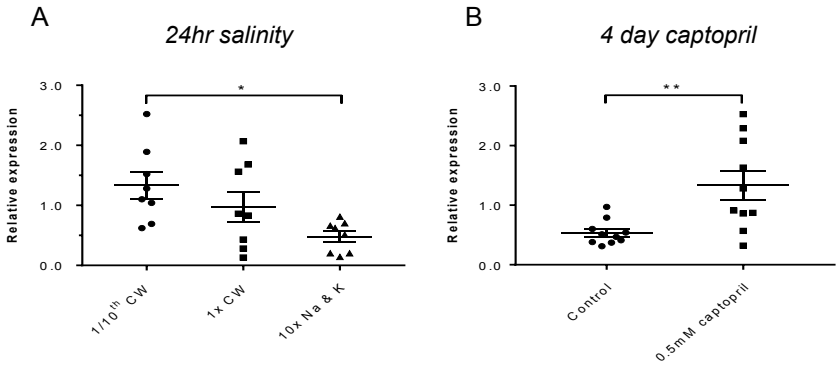
A
24hr salinity
Relative expression
3.0
2.0
1.0
0.0
*
1/10th C:W
1x C:W
10x Na & K
B
4 day captopril
Relative expression
3.0
2.0
1.0
0.0
**
Control
0.5mM captopril

Figure 6

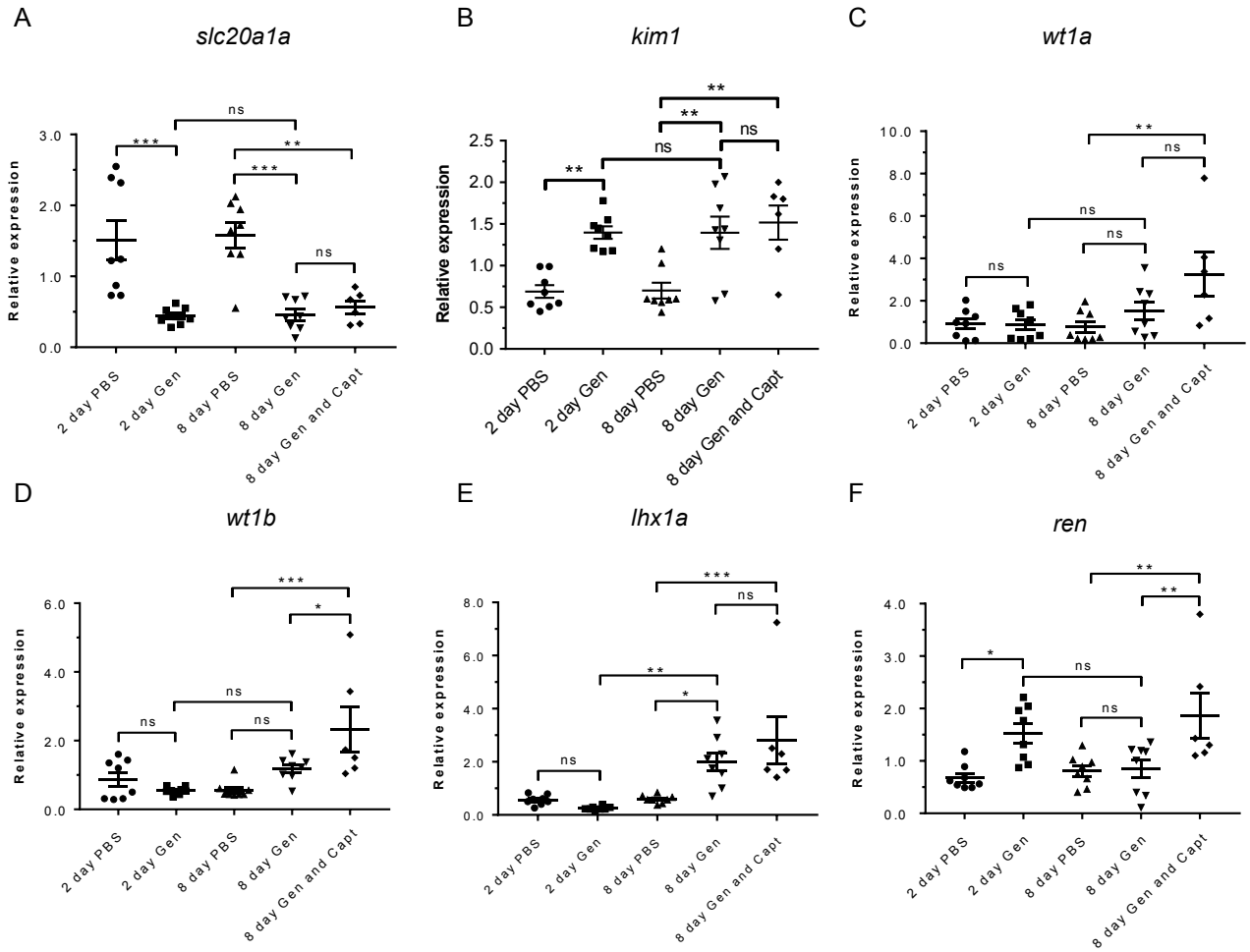
A
slc20a1a
B
kim1
C
wt1a
D
wt1b
E
lhx1a
F
ren
Relative expression
2 day PBS
2 day Gen
8 day PBS
8 day Gen
8 day Gen and Capt
ns

Figure 7

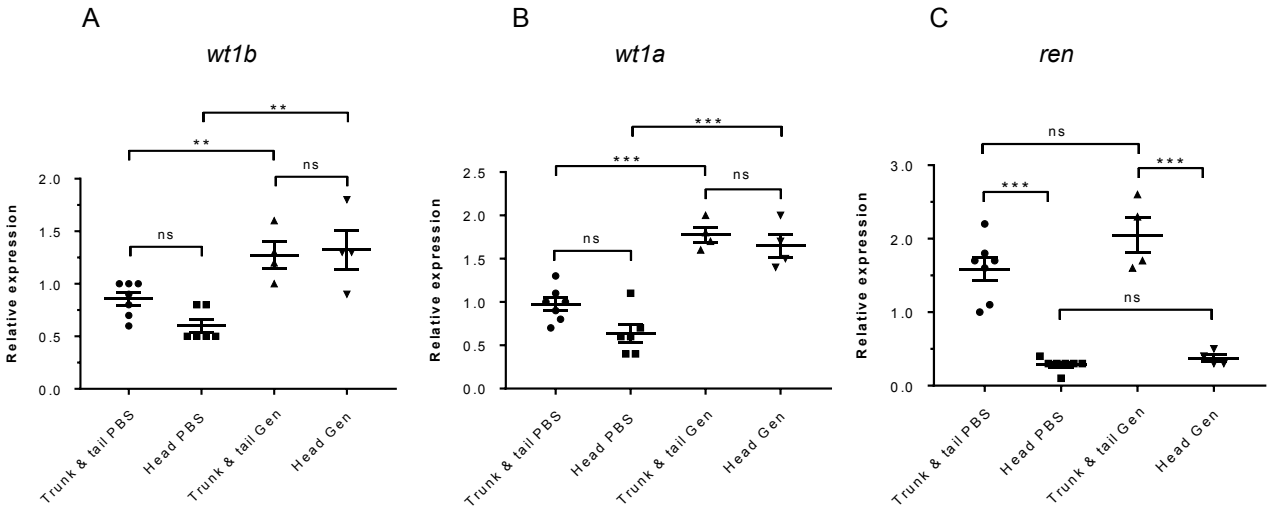
A
wt1b
Relative expression
2.0
1.5
1.0
0.5
0.0
**
**
ns
ns
Trunk & tail PBS
Head PBS
Trunk & tail Gen
Head Gen
B
wt1a
Relative expression
2.5
2.0
1.5
1.0
0.5
0.0
***
***
ns
ns
Trunk & tail PBS
Head PBS
Trunk & tail Gen
Head Gen
C
ren
Relative expression
3.0
2.0
1.0
0.0
ns
***
***
ns
Trunk & tail PBS
Head PBS
Trunk & tail Gen
Head Gen